Response to Referee #2

Thank you for your review of our manuscript. Your comments were well received and will lead to a better paper in response. We will structure our responses as follows: each referee comment will have a number based on referee number and comment from their review. The authors response will be the number with a "R" next to it and changes in the manuscript will be the number with a "C".

2.1 Introduction: in my opinion, the authors should provide a more detailed and comprehensive state of the art of the considered topic. Moreover, they should better emphasize the added-value of their study compared to the previous work.

2.1R - Authors agree. There has been limited peer reviewed articles on this topic. C1 This study will provide an argument for the expanded use of these low cost sensors in science and education. The results on the previous studies will be improved with the comparisons against additional commercial instrumentation, but also through improvements to the processing and analysis. Additional corrections to the wind speed, relative humidity, and solar radiation have been performed improving the overall results. This will also provide the first look at the performance of the UV radiation sensor and its ability to indirectly measure the global downwelling solar radiation.
2.1C - The introduction, station configuration, and results sections will be updated accordingly.

2.2 Station configuration: the authors must provide additional details about technical characteristics of each of the meteorological weather stations involved in this study, the commercial one (Mesonet) and the innovative one (3D-printed). More specifically, I suggest adding a table that list the following specifications: range of measure, resolution, update interval, time-constant and uncertainty (or accuracy). Please consider the following WMO manual as reference: World Meteorological Organization: Guide to Meteorological Instruments and Methods of Observation, 2008.

2.2R - Authors agree. This information has been compiled for both the 3D-printed sensor and the Mesonet sensors. Furthermore, an additional table was developed to compare the accuracy of the reference instrumentation across the previous comparison of the 3D-PAWS stations.

2.2C - Tables 1 and 2 have been updated to gather this information.

2.3 Deployment: According to Table 2, the traditional weather station includes sensors from different commercial companies (Vaisala, RM Young, Met One, Li-Cor). Why did the authors choose a reference meteorological station with these features and with this configuration? From a comparison with standards required by WMO (see Annex 1.E of WMO, 2008), emerges that those sensors are not an adequate and good benchmark to evaluate the performance of the proposed 3D-printed station. For example, according to WMO recommendations, temperature sensor should have an uncertainty of 0.2 K, which is considerable lower than the uncertainty of the RM Young 41342 RTD Probe (0.5 K). This consideration is easily extendable to other "reference" sensors involved in this study, which do not satisfy the WMO requirements. Probably, the authors chose the sensors listed in Table 2 as reference because their accuracy is comparable to that of 3D-printed instruments. However, I am quite skeptical about this approach. At first instance, it may be reasonable, but I think that an additional comparison with sensors that fulfill the WMO standard is necessary, in order to achieve results that are valuable from a "high-level" scientific perspective.

2.3R - This was a low-cost project and access to sensors that fulfill WMO standards while deployed in the field was not possible. The WMO guide does indicate that operational uncertainty conforming to these requirements will not be met in many instances and are only achievable with the "highest quality sensors and procedures". As such, there are a number of organizations that deploy high quality sensors and implement best practices as they relate to calibration and data quality that can serve as viable reference stations. Oklahoma Mesonet sensors undergo routine maintenance and are rotated out of the field on a regular schedule. Calibrations are performed before and after deployment to the field, leading to well-characterized systems. The Oklahoma Mesonet also has a robust data quality program and the data used from their station has been reviewed and properly quality controlled. These sensors were chosen as they were well-maintained sensors that were also accessible to the research team. The 3D Printed weather station was donated to the Cooperative Institute of Mesoscale Meteorological Studies (CIMMS) Education and Outreach program and an additional study will not be possible without building a completely new system. Three of the four authors have also relocated to new positions and funding would need to be secured for another comparison study with sensors meeting WMO standards while deployed in the field.

2.3C - Additional discussion on why these sensors were chosen and how they compare with other studies and the WMO guidelines will be added into the manuscript.

2.4 Moreover, I suggest adding a figure including a photo of Mesonet station facilities. For a reliable comparison, the sensors of the two stations should be installed at the same height above the ground level: as an example, the wind sensors operated at two very different heights (10 m for the Mesonet, 2 m for the 3D-printed station). The authors seem to be conscious of this limit (Lines 85-87), but in my opinion they should discuss this aspect in a more comprehensive manner and should better highlight the limits of their work.

2.4R - Authors agree on adding an additional plot of the Mesonet station. With respect to the wind speed comparisons, a logarithmic wind profile correction was applied to the Mesonet wind speed based on Allen et al 1998. This did bring the Mesonet wind speed values more in line with the 3D printed station for a majority of the deployment.

2.4C - Will add an addition plot of the Mesonet Facility. Authors will also further discuss the differences in the systems and the limits of the comparison.

2.5 Results: the measurements of the two meteorological stations have been compared only in terms of simple scatter plots. It is a very “rudimental”, although useful, analysis. Therefore, I suggest to do more work in this sense: for example, it may be interesting evaluating the performance of the proposed stations as a function of the season and to investigate about the data accuracy in particular “extreme” weather conditions (e.g. strong winds, cold and/or heat waves, strong rainfall, fog, etc.).

2.5R - A more in-depth analysis has been done to calculate standard error of means, root mean square error (RMSE), and also a linear regression including slope, intercept, and correlation. This information along with min/max values for each station are included on the plots. This information was also calculated for each month of the deployment and the RMSE and correlation coefficients were recorded in an additional table. Additional processing has been applied to the relative humidity, solar radiation and wind speeds as well. The relative humidity was corrected using a temperature coefficient correction supplied by the vendor. The solar radiation was measured in counts and a linear regression was performed to convert counts to W/m2. Given the differences in height of wind measurement heights, a logarithmic wind profile conversion was done based on Allen et al 1998. The station was only deployed for 8 months, so more data would be needed to evaluate the performance of the station as a function of season and to further investigate data accuracy in extreme weather conditions. Interestingly, the precipitation gauge performed very well in the one heavier rain event that was encountered. The 3D printed gauge and Mesonet both recorded roughly 104 mm/hr precipitation rate.

2.5C - Authors will update figures with more in depth statistics, summary table of RMSE and correlation coefficient, and additional discussion on results.

2.6 Furthermore, for rainfall data, I suggest to perform a comparison not only in terms of daily accumulated rainfall but also in terms of rain rate.

2.6R- Data were processed for rain rate and will be included in the discussion and results accordingly.

2.6C - Rain rate results will be added to the results section.

2.7 Conclusions: please add an additional discussion about the limits of those preliminary results and about the future planning and evolution of this study.

2.7R - Authors will add additional discussion noting the differences between the systems and the limitations. The future and evolution of this study would have naturally been to extend it to different measurement types (soil moisture, spectral radiation, etc). Two of the authors have/will graduate from the University and the lead author has changed jobs and is now at Argonne National Lab in Chicago which will limit additional comparisons with the Oklahoma Mesonet. However, there still exists some opportunities to further advance this topic and potentially partner with other groups for future studies.

2.7C - Authors will add in addition discussions on the limits of the results and the natural evolution of this study

Response to Referee #3

Thank you for your review of our manuscript. Your comments were well received and will lead to a better paper in response. We will structure our responses as follows: each referee comment will have a number based on referee number and comment from their review. The authors response will be the number with a "R" next to it and changes in the manuscript will be the number with a "C".

3.1 - A more detailed analysis of the comparisons of the low-cost and reference weather stations is necessary in order to show the clear differences between the two instruments, as the study using only scatterplots and average differences appears too raw and limiting. A more detailed and quantitative approach through merit factors (such as error, bias...) would be desirable.

3.1R - Authors agree. Additional processing has been applied to relative humidity, solar radiation and wind speeds. A correction for the temperature coefficient was applied to the relative humidity based on vendor documentation which improved the overall results. The solar radiation was measured in counts and a linear regression was performed to convert counts to W/m2. Given the differences in height of wind measurement heights, a logarithmic wind profile conversion was done based on Allen et al 1998. Using these results, a more in-depth analysis has been performed to calculate standard error of means, root mean square error (RMSE), and also a linear regression including slope, intercept, and correlation. This information along with min/max values for each station are included on the plots. Statistics were also calculated for each month of the deployment and the RMSE and correlation coefficients were recorded in an additional table. Additionally, the performance of the temperature and relative humidity sensors were analyzed with increasing wind speeds to determine the effects the naturally aspirated wind shield would have on the measurements.

3.1C - Updated figures with more in depth statistics, summary table of RMSE and correlation coefficient, summary table of RMSE and correlation coefficient for temperature and relative humidity based on different wind speed thresholds, and additional discussion on results.

3.2. Can be low-cost measurements corrected in some way in order to reproduce reference observations?

3.2R - It would be relevant to run the sensors through calibrations before and after deployment to the field to better characterize the sensors, similar to the Oklahoma Mesonet practice. However this would also add additional expenses. Inaccuracies owing to drift would be harder to compensate for. It is also unknown how the drift rates differ between boards of the same sensor type. Further analysis of the performance of multiple boards of the same sensor would be necessary to better characterize them. As mentioned in 3.1R, the relative humidity, solar radiation, and wind speed measurements were corrected, which produced improved results.

3.2C - Where relevant, the result discussion was updated with the corrected data.

3.3. Are there some meteorological situations/events in which the low-cost station performs best?

3.3R - Through the added analysis, it was determined that the temperature sensors had improved performance with increasing wind speed, which is expected as the flow through the radiation shield would be more comparable to the Mesonet aspirated radiation shields. The relative humidity did not see the same improvement in performance which could be related to dust collection on the filter on the sensor. While the filter on the sensor was hydrophobic, the dust that collected on it may have not been. The relative humidity did perform better in drier conditions which is expected based on the reduce vendor stated accuracy for the lower to mid ranges of relative humidity. Overall though, more data over repeated seasons would be necessary to determine which conditions/events the station performs best in.

3.3C - Manuscript results discussion was updated with some of this additional analysis.

3.4. It is not very clear how the UV data of the two stations were compared, as it stated in the paper that they do not measure the same radiative components.

3.4R - The UV sensor calculates the UV index by measuring visible and infrared light. This is stored as counts in the data files. It was determined that some other sensors did provide equations to calculate lux from which the W/m2 could be estimated, the sensor used in this study did not. Authors initially used the visible counts to compare with the downwelling global solar radiation but the errors reported would not be informative. To improve on the analysis, a linear regression was performed on the entire dataset and a slope/intercept was applied to the data to make the measurements comparable.

3.4C - Manuscript discussion on the radiation results, solar radiation plot, and statistics will be updated with the new results.

3.5. I think a table summarizing all the sensor differences/performances would be valuable to have a clear picture of the comparisons.

3.5R - Authors agree.

3.5C - Table 4 will be included with summary of RMSE and correlation coefficient for all measurements for each month and for the entire campaign. This is also relevant to updates made in Table 1 and Table 2 to better follow WMO guidelines on reporting range, resolution, accuracy, and more. Table 3 was added to give an overview of the specific measurement accuracy of the reference sensors used thus far in all comparisons with 3D-PAWS.

3.6. The comparison between the two rain gauges should be expanded: how the two instruments work on the basis of rain rate?

3.6R - Both rain gauges are tipping bucket gauges with the 3D printed rain gauge performing a tip for every 0.2 mm while the Mesonet bucket tips on 0.254 mm. The white Mesonet gauge is located 0.6 m off the ground and is surrounded by an alter shield to decrease the wind effects. The gray 3D weather station gauge was roughly 0.3 m off the ground and was not surrounded by an alter shield. The color of the gauges are noted as neither gauge has a heater and how the different gauges heat up following a solid precipitation event could impact the rain rates recorded.

3.6C - Manuscript will be updated to include this relevant information and expand on it. Minor Comments

3.m1 - Do you have any idea about the duration of 3D-printed weather station and its sensors without any maintenance located, for example, in a remote area?

3.m1R - Based on our experience, the durability of the 3D printed parts varied. Printed parts used in the wiring of the station such as the nuts for tightening instruments in place, for example, would have a low life expectancy without proper maintenance. The durability of the wiring connectors was inconsistent due to minor imperfections caused by the printing process. These imperfections forced excessive filing of the wire connectors in order to securely fit wiring. Connectors that were excessively filled often wore down to the point where wiring had difficulty remaining in the connector itself. Nuts tended to lose grip over time causing the instruments to sag or rotate in their housing. Parts with constant friction, like the anemometer, would have lower expected life spans. Most of the parts that did not fall under these previous examples remained in very good condition at the conclusion of the deployment. Sensor longevity seemingly was related to whether the sensor could be impacted by the outside elements, namely moisture. The temperature, humidity, and pressure sensors housed in the radiation shield showed varying degrees of corrosion throughout the study, with the humidity sensor ultimately having to be removed. The rain gauge and wind sensors, which were more sheltered from the outside conditions, showed no evidence of degradation at the conclusion of the study. If we were to recreate this system again, the wiring connectors would be the main area of improvement sought as a lot of time was spent working on these connections. The fitting to secure the wind direction vane would be second as the results were not ideal as it kept coming loose and rotating from truth North orientation.

3.m1C - Manuscript section discussing the 3D printed components will be updated with some additional information.

3.m2 Line 64: the average difference of air temperature is 0.81, while the related scatterplot indicates 0.82

2.m2R - Thank you for noting this. The more in-depth analysis has produced some updated results and the manuscript will be updated accordingly.

Changes to Manuscript

Based on the referee comments, major revisions were made to the manuscript. This included updates to all sections. An overview of the updates are noted below, followed by the full paper showing differences as detected by latexdiff.

- Introduction
  - Major additions to better scope the relevance of this work along with introducing the reference instrumentation a little more.
- Station Configuration
  - The deployment section was split out and added to introduction and station configuration
  - Additional information was added to the station configuration section to denote the differences in the 3D-printed system vs the Oklahoma Mesonet.
- Results
  - Results were completely rewritten to include additional analysis that was request, including RMSE, Correlation Coefficient, and more.
- Discussion
  - Discussion was updated based on new and improved results
- Appendix A
  - Added to better document the instrumentation used in previous comparisons using the 3D-PAWS system
- Figures
  - All graphs where updated with new results
  - Image of the Norman Mesonet site was added
- Tables
  - Table 1 was updated to include instrument specifications for the 3D-PAWS sensors
  - Table 2 was updated to include additional instrument specifications from the Mesonet station
  - Table 3 was added to show the reference instrument accuracies from past 3D-PAWS studies
  - Table 4 was added to reference RMSE and correlation coefficient for each month of the deployment and then overall values
  - Table 5 was added to document the effects of wind speed on the temperature and humidity results
  - Table 6 was added to document the instrument performance as it relates to rain accumulation and rain rate through the deployment.

More Science with Less: Evaluation of a 3D-Printed Weather Station

Adam Theisen[1,2], Max Ungar[1], Bryan Sheridan[1], and Bradley G. Illston[3]

[1]Cooperative Institute for Mesoscale Meteorological Studies, University of Oklahoma 120 David L. Boren Blvd., Suite 2100 Norman, OK 73072

[2]Argonne National Laboratory 9700 S Cass Ave, Lemont, IL 60439

[3]Oklahoma Mesonet, University of Oklahoma 120 David L. Boren Blvd., Suite 2900 Norman, OK 73072

Correspondence: Adam Theisen (atheisen@anl.gov)

Abstract. A weather station built using 3D-printed parts and low-cost sensors, based on plans and guidance provided by the University Corporation for Atmospheric Research 3D-Printed Automatic Weather Station Initiative, was deployed alongside an Oklahoma Mesonet ~~Station for an eight month study to~~ station to compare its performance against standard commercial sensors and determine the longevity ~~of these sensors and their performance as compared with standard commercial sensors . The station was built based on plans and guidance provided by the UCAR 3D-PAWS project. While some of the sensors and components did degrade over time and in some cases completely fail, the~~ and durability of the system. Temperature, relative humidity, atmospheric pressure, wind speed and direction, solar radiation, and precipitation measurements were collected over an eight-month field deployment in Norman, Oklahoma. Measurements were comparable to the commercial sensors except for wind direction, which proved to be problematic. Longevity and durability of the system varied, as some sensors and 3D-printed components failed during the deployment. Overall, results show that these low-cost sensors ~~have the potential to perform just as well as~~ are comparable to the more expensive ~~counterparts~~commercial counterparts and could serve as viable alternatives for researchers and educators with limited resources.

1 Introduction

Low-cost sensors~~coupled with 3D-printing~~ , coupled with three-dimensional (3D) printing technologies, can provide researchers and educators with the ability to create tools and instrumentation at a fraction of the cost of commercial counterparts. The 3D-Printed Automatic Weather Station (3D-PAWS) Initiative ~~developed open-source plans and documentation for building low-cost weather stations~~ was launched by the University Corporation for Atmospheric Research (UCAR) and the US National Weather Service International Activities Office, with support from the USAID Office of U.S. Foreign Disaster Assistance, in an effort to fill observational gaps in remote, sparsely observed regions ~~(Kucera and Steinson, 2017b). There have been similar~~ (Kucera and Steinson, 2017a). Scientists behind the 3D-PAWS Initiative developed and open-sourced robust plans, documentation, and software for the development of a 3D-printed weather station capable of measuring temperature, humidity, atmospheric pressure, ultraviolet (UV) index, wind speed and direction, and rainfall using low-cost commercially available sensors (Table 1). Similar efforts to develop low-cost weather stations have emerged for small-scale wind farm site selection (Aponte-Roa et al., 2018) and ~~for looking at~~ investigating micro-climate processes (Ham, 2013). ~~Other than the~~

~~3D-PAWS experiment, these efforts along with independent ones (Smallwood and Santarsiero, 2019)~~ In addition to weather stations, efforts are expanding towards the creation of other low-cost sensors that could benefit environmental and atmospheric science applications (Ham et al., 2014; Kennedy, 2019). Most efforts related to weather station development have focused on relatively short time periods for ~~validation~~ evaluation of the sensors and 3D-printed components, however, the 3D-PAWS Initiative has tested and deployed their systems in a long-term operational manner, with approximately nineteen stations deployed worldwide (Kucera and Steinson, 2017a).

Evaluation of these low-cost systems against commercial grade instrumentation is important in proving these technologies and enabling adoption on a wider scale. The 3D-PAWS ~~team evaluated their system~~ system has thus far been evaluated against all-in-one (Smallwood and Santarsiero, 2019; Aura et al., 2019) and commercial grade sensors (Kucera and Steinson, 2017a). Smallwood and Santarsiero deployed a complete station, but only collected a limited amount of data due to data acquisition issues and an analysis was not performed. Aura et al. compared three years of 3D-PAWS data with an all-in-one weather station and found high correlation for atmospheric pressure, moderate correlation for temperature, relative humidity, and wind direction and relatively low correlation for wind speed. Additionally, Aura et al. concluded that routine maintenance was important for these automated weather systems to ensure data availability and quality. 3D-PAWS developers evaluated their system against high quality sensors over a ten month time-frame ~~at two separate facilities, each having commercial grade sensors for comparison (Kucera and Steinson, 2017c). The results~~ in Boulder, Colorado, in an environment where temperatures ranged from approximately -25 °C to 37 °C and at the National Oceanic and Atmospheric Administration (NOAA) testbed facility in Sterling, Virginia (Kucera and Steinson, 2017a). Results showed good agreement between sensors~~with the relative humidity showing the largest uncertainty (Table: **??**). Other than the Smallwood and Santarsiero study, which did not gather enough data for analysis, each effort found that these low-cost sensors can be a viable alternative for data collection.~~ , with most sensor uncertainty falling within range of the manufacturer specifications. The exception was relative humidity which had a higher uncertainty of 5.7 % (Table 1). Performance of the UV sensor was not assessed in previous comparison studies.

Accurate reference sensors are essential for proper comparisons. Ideally, reference sensors would conform to standards defined in World Meteorological Organization (WMO) Guide to Instruments and Methods of Observation (WMO, 2018). However, the WMO guide also indicates that operational uncertainty conforming to these requirements will not be met in many instances and are only achievable with the "highest quality sensors and procedures". There are a number of organizations that deploy high quality sensors and implement best practices as they relate to calibration and data quality that can serve as viable reference stations. The Oklahoma Mesonet (Mcpherson et al., 2007; Brock et al., 1995), hereafter referred to as Mesonet, deploys high quality meteorological instrumentation (Table 2) in every county across Oklahoma. Mesonet sensors undergo routine maintenance and are rotated out of the field on a regular schedule. Calibrations are performed before and after deployment to the field, leading to well characterized systems (Mcpherson et al., 2007). The accuracy of the Mesonet sensors are comparable to Kucera and Steinson, with noticeable improvements over the all-in-one sensors used in the Smallwood and Santarsiero and Aura et al. studies (Table 3). Information about the particular sensors used in each of these studies is documented in Appendix A.

This study was supported by a grant through the Cooperative Institute ~~of~~ for Mesoscale Meteorological Studies (CIMMS) at the University of Oklahoma with the ~~goal~~ goals of verifying the ~~3D-PAWS results , determining~~ results from previous inter-comparison studies, assessing the longevity of the sensors and 3D-printed components, and most importantly, providing undergraduate meteorology students with skills they would not otherwise have learned in the classroom. Through this project, students were able to gain valuable hands on experience with proposal writing, project plan development, 3D printing, instrument engineering and development, and field campaign operations.

2 Station Configuration

The weather station was built based on specifications provided by the 3D-PAWS ~~initiative~~ Initiative with some modifications. ~~Due to~~ Over 100 parts were 3D-printed using off-white acrylonitrile styrene acrylate (ASA), which has higher ultraviolet radiation, temperature, and impact resistance than regular polylactic acid (PLA) filament. Parts were printed with a grid infill to reduce printing time. ASA is printed using higher temperatures than standard PLA filament, which can lead to warping of prints, as was the case for the radiation shield leafs. Initial prints of the rain gauge funnel using the original design proved problematic with the printer used. The wall thickness of the funnel was increased to resolve the print issues. Due to a vendor shortage of the original off-white ASA, the funnel was printed with gray ASA. It was coated with polyurethane to seal any remaining imperfections in the print. Lab calibrations of the rain gauge were performed and it was adjusted to ensure that each tip routinely held 0.2 mm of water compared to 0.254 mm for the Mesonet rain gauge. The rain gauge screen was created using parts from a failed funnel print. Mosquito netting was zip tied to the ring and placed securely inside the funnel. Plans provided by the 3D-PAWS Initiative called for opaque plastic (PTFE) to shield the UV sensor. In order to reduce costs, an opaque plastic tray from a frozen meal was used to create the UV sensor cover (Fig. 1). Temperature, relative humidity, atmospheric pressure, and UV sensors were all sealed with conformal coating to protect against degradation due to moisture.

Due to limitations with anchoring the station in ground, a frame had to be developed to withstand weather conditions in Oklahoma. The frame was built from standard polyvinyl chloride pipe (PVC) and consisted of a central trunk connected to three legs ~~.~~ (Fig. 2). Each leg was connected to a height adjustable concrete footing~~(Fig. 2).~~. In order to minimize vibrations on the tipping bucket rain gauge, the support legs were also set in concrete. In ~~place~~ lieu of building a Raspberry Pi tube, an ~~eight by eight by four inch~~ electrical junction box was used to house the Raspberry Pi. Temperature, relative humidity, and atmospheric pressure sensors were installed in the naturally aspirated radiation shield at ~~one-and-a-half meters~~ 1.5 meters to match the height of the Mesonet. Wind direction, wind speed, and ~~ultraviolet (UV)~~ UV light sensors were installed on the crossbar at approximately two meters ~~.~~ compared to ten meters for the Mesonet wind measurements. The tipping bucket rain gauge was installed at roughly 0.3 meters compared to 0.6 meters for the Mesonet. A secondary temperature sensor was installed in the Pi box to monitor internal temperatures. ~~Temperature~~

Software provided by the 3D-PAWS Initiative was not compatible with the raspberry Pi version used for this study and additional software engineering was required. Existing python libraries were used for communications with temperature

(DiCola, 2014b), relative humidity (Gaggero, 2015), atmospheric pressure (DiCola, 2014a), and UV ~~sensors were all sealed with conformal coating to help protect against moisture degradation.~~

~~Over one hundred parts were 3D-printed using acrylonitrile styrene acrylate (ASA) which has higher ultraviolet radiation, temperature, and impact resistance than regular polylactic acid (PLA) filament. In order to print the parts in a timely manner, the parts were not completely filled in and instead were printed with a grid infill. Initial prints of the funnel using the original design proved problematic with the printer that was being used. The wall thickness was increased to resolve the print issues. The funnel was coated with polyurethane to seal any remaining imperfections in the print. Lab calibrations were performed and the rain gauge was adjusted to ensure that each tip routinely held approximately 0.2 mm of water. The rain gauge screen was created from part of a failed funnel print. Mosquito netting was zip tied to the ring and fit securely inside the funnel. Plans had called for opaque plastic (PTFE) to shield the UV sensor. In order to reduce costs, the opaque plastic tray from a frozen meal was used to create the cover (Fig. 1).~~

light sensors (Gutting, 2014). The 3D-PAWS software image was decoded and used as a basis for the wind and rain programs. Data were collected instantaneously every minute for ~~the~~ temperature, pressure, relative humidity, and UV variables. The rain program was constantly listening for tip events and ~~would record minute totals~~ recorded event totals every minute. The wind program was constantly running as well~~and recorded~~, taking measurements every ten seconds and recording average, minimum, and maximum wind speed and direction ~~each minute. These programs~~ every minute. Programs were set up to automatically start up on any reboot or power loss event to ensure robust operations. Data were automatically uploaded via WiFi connection to a cloud based storage location at the end of every day (24:00:00 UTC) to ensure minimal data loss in the event of a catastrophic failure.

3 ~~Deployment~~

~~The Oklahoma Mesonet (Mcpherson et al., 2007; Brock et al., 1995) deploys meteorological instrumentation (Table: 2) in every county across Oklahoma. Temperature, pressure, and relative humidity sensors are deployed at one-and-a-half meters and the wind speed and direction at ten meters.~~ The 3D-printed station was deployed approximately seventy meters to the West-Northwest of the Norman Oklahoma Mesonet station (Fig. 3) The Norman station (Fig. 4) served as an ideal reference point due to the proximity to the University of Oklahoma for easy installation and routine maintenance visits. Power was also easily accessible, eliminating the need for solar panels and batteries. The 3D-printed ~~weather station was deployed approximately seventy meters to the West-Northwest of the Mesonet station (Fig. 3). The wind sensor~~ station cross-arm was ~~mounted~~ oriented perpendicular to North ~~and~~ with the rain gauge ~~was oriented~~ positioned to the West of the station in order to minimize any interference from the station itself or the larger ten meter tower ~~that was nearby. There was a slight slope to the terrain so~~ nearby. The terrain of the site was slightly sloped such that the 3D-printed ~~weather~~ station was approximately two meters higher than the Mesonet ~~site. Surrounding terrain~~ station. Surrounding vegetation was mostly native grasses~~that~~, which were mowed on a regular basis.

3 Results

Temperature, relative humidity, atmospheric pressure, wind speed and direction, and UV data collected from the 3D weather station were averaged to five minutes in order to compare with the Mesonet data ~~.~~ downloaded from Atmospheric Radiation Measurement User Facility (ARM, 2019). The Atmospheric data Community Toolkit (Theisen et al., 2020) was used to read in the different data formats into common xarray objects for analysis (Hoyer and Hamman, 2017). The ~~Mesonet does not measure UV index so a one-to-one comparison was not possible. Rainfall from both systems were accumulated to a daily total for comparison. Results across the various sensors are mixed, but overall the station exceeded expectations. The~~ subsequent scatter plots, produced using Matplotlib (Hunter, 2007), follow the same format, the ~~3D weather station is~~ 3D-printed station is displayed on the x-axis ~~,~~ and Mesonet on the y-axis~~, and the points~~. Points are color-coded by ~~time~~ a consistent time interval, 15 August 2018 to 15 April 2019, with dark blue indicating data ~~from~~ collected towards the beginning of the deployment and yellow indicating data collected towards the end of it. A one-to-one line is indicated by the blue dashed line. The solid black line denotes the linear regression calculated using SciPy (Virtanen et al., 2020). Slope, intercept, and correlation coefficient are listed on the bottom left. Standard error of the mean (SEM), root mean square error (RMSE), average difference, and minimum and maximum values of the 3D-printed station and Mesonet are listed in the lower right. A summary of the RMSE and correlation coefficients broken down by month and for the full deployment is in Table 4.

3.1 Air Temperature

~~The MCP9808 temperature sensor differed from the RM Young probe by an average of 0.81~~ Air temperature data were quality controlled by applying an upper threshold of 45 °C ~~which is within the range of uncertainty of both instruments combined (0.5~~ to the 3D-printed station temperature data in order to remove erroneous data points. The Mesonet data had been properly quality controlled and no further quality control was necessary. The MCP9808 sensor reported large values towards the end of the deployment, but otherwise performed well with a RMSE of 1.22 °C when compared with the Mesonet sensor (Fig. 5). The lowest RMSE value (0.42 °C~~and 0.4~~) was recorded in month seven immediately before the sensor began to fail, which resulted in an RMSE of 1.53 °C ~~)~~for month eight (Table 4). Temperature sensors were also incorporated into the HTU21D relative humidity and BMP280 atmospheric pressure sensors. Temperature from the BMP280 sensor was not included in the analysis due to the sensors subsequent relocation inside the Raspberry Pi box. Temperature reported by the HTU21D sensor performed better than the primary MCP9808 sensor, with an overall RMSE of 0.97 °C (Fig. ~~5). The slight differences could also be attributed to the difference in aspiration, natural vs mechanical. The low-cost~~ 6). However, the HTU21D sensor failed in the sixth month of the deployment. This failure was attributed to corrosion on the board that was not observed amongst the other sensors. The MCP9808 sensor did show some signs of degradation at the end of the deployment due to moisture but was otherwise in relatively good shape.

~~A temperature sensor was also incorporated in the~~ Differences in the radiation shield configuration between stations contributed to a portion of the observed differences. The Mesonet deploys actively aspirated radiation shields, while the 3D-printed station radiation shield was naturally aspirated. Data were additionally analyzed by applying thresholds to the data based on wind speeds from 1 m s^{-1} to 8 m s^{-1}. RMSE significantly improved for the MCP9808 sensor, from 1.22 °C to 1.08 °C with a threshold of 1 m s^{-1} and from 0.97 °C to 0.91 °C for the HTU21D sensorused for relative humidity. The HTU21D outperformed the . RMSE continued to decline with increasing wind speeds for both sensors (Table 5). As flow through the naturally aspirated radiation shields increased, it became comparable to the flow through the Mesonet aspirated radiation shields. The RMSE of both sensors are inline with the sensor uncertainties between both stations (MCP9808 when compared to the Mesonet (Fig. 6) , however, 0.8 °C; HTU21D 0.6 °C) when the wind speeds are greater than roughly 5 m s^{-1}.

3.2 Relative Humidity

As mentioned in the previous section, the HTU21D failed two-and-a-half months before the end sensor failed in month six of the deployment. This failure was attributed to corrosion on the board that was not seen with other sensors.

3.3 Relative Humidity

The HTU21D relative humidity sensor had a , but was able to measure a broad range of relative humidity values from 11 % to 100 % (Fig. 7). Corrections were applied using a manufacturer supplied temperature coefficient compensation equation with a temperature coefficient of -0.15 % RH/°C (Inc, 2013). Values above 100 % were set to 100 %, following the Mesonet practice (Mesonet, b). RMSE for the entire campaign was 3.33 %, indicating a slight moist bias as compared to the Mesonet's Vaisala HMP155 probe, averaging 4.2 %(Fig. 7) with the low-cost sensor. Prior to applying the manufacturer correction, the overall RMSE was 5.00 %. The bias increased with increasing relative humidity . To elaborate on the previously mention failure of the HTU21D sensor, communications problems started roughly five-and-a-half months into the deployment. These communications problems caused readings from other sensors using the same protocol (I2C) to drop out. The HTU21D sensor was removed and notreplaced due to the short amount of time remaining in the deploymentsensor specifications indicate that uncertainties are larger for relative humidity measurements greater than 80% (Table 1). However, the RMSE was little changed (0.09 %) when data above and below this limit were excluded from the analysis. When this limit was lowered to 50 %, relative humidity values over 50 % had an RMSE of 3.44 % compared to 2.42 % under 50 %. Unlike the RMSE of temperature, the relative humidity RMSE was relatively constant with increasing wind speed thresholds (Table 5). A polytetrafluoroethylene (PTFE) filter covered the sensor to keep it clean and appeared to have some staining when the sensor was uninstalled from the station. The filter itself was hydrophobic, but it is possible that the accumulated dust on it was not. Overall, the observed errors between the systems were comparable to the sensor accuracy across relative humidity values.

3.3 Atmospheric Pressure

The initial BMP280 pressure sensor that was deployed with the station had large errors when compared to the Mesonet. The replacement sensor suffered from communications A replacement sensor was installed but suffered from communication problems owing to bad wire connections and was moved from the radiation shield to inside the Raspberry Pi box. The assumption was that there would be minimal difference owing in pressure measurements due to the openness of the PVC frame and that the connection to the radiation shield which would allow for proper air flow for atmospheric pressure measurements. The Temperature in the box varied but did not appear to greatly affect the measurements, as the RMSE of the pressure was fairly constant for the entire deployment with an overall RMSE of 2.39 hPa (Table 4). There was very little deviation in the measurements and it appears that the BMP280 sensor also had a temperature sensor, but this move to the logger box invalidated the results. The BMP280 pressure compared well with the Mesonet's Vaisala Barometer with a consistent bias of 2.35 hPa (sensor has a nearly constant offset when compared to the Mesonet (Fig. 8).

3.4 Wind Speedand Direction

In order to properly compare the ten meter Mesonet wind speeds to the 3D-printed station two meter winds, a logarithmic wind profile was assumed and the ten meter Mesonet winds were adjusted based on the method from Allen et al. (1998). The resulting conversion factor, 0.748, was applied to the Mesonet wind speed data. Performance over the first three months was comparable to the Mesonet station with an RMSE between 0.56 m s^{-1} and 0.59 m s^{-1} (Table 4). RMSE slowly increased over the course of the deployment, with marked increase in month seven to 2.49 m s^{-1}. This shift in performance is clearly noticed in Figure 9, as the data towards the end of the deployment (yellow) show more of an exponential relationship. A procedure was not in place to routinely clean or oil the bearing, so the gradual rise in RMSE over the deployment could be due to the accumulation of dust. Towards the end of the deployment the anemometer head completely shearing off from the driveshaft, resulting in measurements of 0 m s^{-1} for an extend period of time. This failure could be attributed to two factors. The first factor being the reduced infill used to print the parts in order to save time, which would have weakened the overall strength of the components. The second factor is how the anemometer was built. Initially the anemometer had a large amount of wobble. This wobble was greatly reduced before deployment but not completely eliminated and could have put added strain on the driveshaft.

3.5 Wind Direction

The 3D-printed anemometer had a slow bias throughout the deployment as compared with the Mesonet's RM Young wind monitor. A portion of this could be attributed to the difference in height, ten meters for the Mesonet and two meters for the 3D printed station, but the method for printing and the bearing used likely had a larger impact. The 3D printed anemometer averaged a difference of 1.6 m/s with a larger shift in the bias occurring six-and-a-half months into the wind vane was problematic for the entire deployment (Fig. 9). The anemometer started to degrade and completely sheared off a month later. 10). While there was adequate agreement at times, the RMSE was large and the correlation coefficient was not ideal (Table 4). The 3D-printed wind vane was held accurately inline with true North by a 3D-printed clamp and bolt. The This clamp and bolt routinely loosened over time causing the direction to drift throughout the entire deployment. The alignment was check checked and adjusted with each maintenance visit, but was short-lived. While there was good agreement at times (Fig. 10), the majority Throughout the deployment the wind vane tended to stick in certain directions. Efforts were taken to reduce the sticking, but it proved to be an issue for most of the deploymentwas out of sync with the Mesonet. Additionally, a by-product of 3D printing this piece was small grooves in the wind vanewhich created a , a byproduct of the 3D-printing process, created an ideal location for insects to lay eggs. large numbers of eggs. This natural factor may have added to data quality issues towards the end of the deployment as well.

3.6 Solar Radiation

While the SI1145 sensor and the Mesonet's Li-Cor Pyranometer did not measure the same radiative components, the components they did measure were comparable The Mesonet measured downwelling global solar radiation and the UV sensor measured counts of visible and infrared light in order to calculate a UV index. It was discovered that similar UV sensors from other manufacturers provided coefficients for calculating lux from their sensors, which could then be converted to W m^{-2}. However, no such coefficients were found for the SI1145 sensor. There was a linear correlation between the downwelling global measurements and the visible counts (Fig. 11). It is reasonable that a retrieval could be calculated in order to convert the counts to W/m^2. The , so a simple linear regression was performed to determine the slope (0.70) and intercept (170.66) of the data for the entire deployment. These values were applied to the counts data to make it comparable with the Mesonet measurements.

The SI1145 UV sensor had a high bias for the initial few months of the deployment and a low bias for the latter months. The sensor was difficult to keep perfectly level and was routinely adjusted during maintenance visits. The plastic disc held up to the elements but the glue used to seal it yellowed . over time (Fig. 1). 3D-printed connectors routinely lost physical connection to the UV sensor and tape had to be applied to hold it together. The tape did not completely fix the issue as their were intermittent outages resulting in intermittent outages throughout the deployment. The levelness of the sensors, yellowing of the glue, and intermittent outages contributed to the changes observed in RMSE throughout the deployment (Table 4).

3.7 Precipitation

Efforts to increase the sturdiness of the funnel failed rain gauge funnel failed, as the funnel had broken broke off at the neck on the initial installation. A thick layer of silicone caulk was applied to the break , ensuring that opening stayed while ensuring that the opening remained clear. The funnel was planned to be replaced on upon failure, however, that failure did not occur. The 3D-printed rain gauge performed surprisingly well in liquid precipitation events as compared with the Mesonet 's MET One tipping bucket rain gauge early on in the deployment compared to the Mesonet (Fig. 12). and 13). Daily accumulations and rain rates compared well with the Mesonet for the first few months (Table 4). The 3D-printed rain gauge performed very well during a heavy precipitation event in month five, measuring a rain rate of 103.2 mm hr^{-1} compared with the Mesonet rain rate of 103.7 mm hr^{-1} (Table 6). Very poor correlation coefficient and low RMSE in month six can be attributed to the limited precipitation recorded for that period of time, with a maximum accumulation of 2.2 mm during that period. The rain gauge tended towards a high bias in months seven and eight, the cause of which is unknown but assumed to be related to its subsequent failure. The nut holding the rain gauge had come loose at some point loosened towards the end of the deployment and the rain gauge had disconnected and fallen offeventually the wiring disconnected resulting in a number of missed events. Neither the Mesonet nor the 3D-printed rain gauge were heated, so the differences in precipitation measured during solid precipitation events could be attributed to different melt rates between the gauges. The funnel rain gauge was printed with gray filament due to limited supplies of the white ASA filament and was ~~more~~ further exposed to the environment than the Mesonet gauge, both of which could contribute to different melt rates.

3.8 ~~3D-Printed Components~~

4 Conclusions

While the sensors used as a reference were not up to WMO standards, they were very well maintained and characterized, leading to high confidence in the reference measurements and results. Though there were a number of differences in the physical deployment of the systems, the temperature, relative humidity, atmospheric pressure, wind speed, and precipitation sensors all performed reasonably well for a majority of the campaign with relatively lower RMSE and higher correlation coefficients observed in comparisons with the Mesonet system. Decreasing RMSE for temperature with increasing wind speeds reveals the effect of the different types of radiation shields. The addition of a miniature five volt fan to the radiation shield to increase airflow could improve the overall temperature and relative humidity measurements, but would add additional strain to the system if operating remotely on solar and battery power. Wind measurements were taken at two different heights, with the Mesonet wind speed adjusted using an assumption that the wind profile was logarithmic. This assumption may not hold in more complicated terrain where these systems are sometimes deployed. Additional work is need to determine the feasibility of deploying wind sensors at ten meters as it would put added stress on the frame and potentially increase the risk of failure to the entire system. Disappointing results from the wind vane can be attributed to the bearing, but also indicates that a more robust solution is needed to ensure the sensor stays oriented with true North. Measurements from the solar radiation sensors were of different components which is not ideal from a comparison standpoint, even though the results were generally positive. Depending on the needs of the project, different lux sensors could be deployed in place of the UV sensor.

As previously mentioned, some of the 3D-printed components failed (anemometer, rain gauge funnel) or routinely disconnected (UV sensor) but overall the components and the frame held up well to the environmental stresses. The decision to reduce the print quality by decreasing the infill ~~and increasing the layer diameter~~ did have a negative impact on some of the components ~~. Issues with the wind speed could potentially be attributed to the sturdiness and density not being the same as that of the original design. Water did intrude~~ but in general, the majority performed as expected. Water intruded into the PVC cross-arm ~~, but a few select holes were made to drain the water and no water damage was observed~~through the physical connectors between the 3D-printed parts and the PVC frame. Applying silicone to these areas and drilling holes in the PVC frame alleviated water intrusion and accumulation. Holes were initially drilled into the elbow leading into the Raspberry Pi box to prevent water intrusion and worked as expected. In order to account for the additional temperature sensor in the Raspberry Pi box and the eventual relocation of the pressure sensor there as well, block connectors were utilized to simplify connections. These block connectors could easily replace the 3D-printed common rail assemblies in order to reduce the assembly time and ensure more reliable connections. The frame and sensor housings that made it to the end of the deployment were donated to the ~~Cooperative Institute for Mesoscale Meteorological Studies (CIMMS)~~ CIMMS education and outreach group.

~~Results showed~~ Overall, the results are positive and indicate that many of these ~~low-cost sensors , temperature, pressure, rain gauge, UV, and relative humidity,~~ low cost sensors and the 3D-printed housings can be viable options for gathering meteorological ~~datasets when the commercial sensors are too cost prohibitive. The wind sensors did prove problematic, but could be improved with better print quality and different bearings. With the exception of~~ data when the cost of commercial sensors is prohibitive. Comparisons, such as this, will improve the understanding of how well these low-cost sensors can perform, their longevity in the field, and the ~~anemometer shearing off and the rain gauge joint coming lose, the ASA filament did withstand the elements. It is important to note, that while the reduction in print quality did not negatively affect many of the components, there are some where it did to the point of failure. The frame, while not aesthetically pleasing, proved to be extremely sturdy and durable and will continue to serve as mechanism for education and outreach.~~ long-term resource requirements and maintenance schedules for these types of systems. Capabilities in the area of low-cost sensors are constantly expanding, as is the possibilities for new advancements with other measurements. Subsurface, spectral solar radiation, and aerosol measurements are examples of areas that could benefit from the broader use of low-cost sensors. However, in order to enable wider adoption of these technologies, they must be vetted by the community to ensure that the measurements they provide are comparable to that of industry standard sensors.

Code and data availability. Code and data used on the 3D-printed weather station and for the subsequent analysis are available at https://github.com/AdamTheisen/3DWxSt (Theisen, 2019)

Appendix A: Reference Instrumentation

The type and configuration of the sensors used as a reference for the 3D-PAWS comparison studies have varied. This appendix is to document the reference sensors of previous studies and the configurations of those systems if known.

A1 Smallwood and Santarsiero

Smallwood and Santarsiero used an AcuRite Pro Model 01024 all-in-one weather stations as a reference station. Documentation indicates that barometric pressure is measured but does not list the accuracy of the measurement (AcuRite, 2019). The sensor uses a cup and vane to measure wind speed and direction but is also only capable of measuring sixteen points of wind direction which is why accuracy was left out of Table 3.

A2 Aura et al.

Aura et al. used an ATMOS41 deployed as part of the Trans-African Hydro-Meteorological Observatory as a reference station. The system does not have moving parts so the wind measurements are from acoustic sensors at two meters. Likewise, the rain gauge sensor uses a drip counter made of gold electrodes (METER Group Inc, 2017a, b).

A3 Kucera and Steinson NCAR Testbed

The NCAR Marshall Field Site used in Kucera and Steinson housed a variety of sensors. Temperature and humidity were measured with a Campbell Scientific 500 Series Sensor. The NCAR field site website points to a Campbell Scientific HC2S3-L probe being used and the accuracy specifications from that sensor were used (Scientific, 2020). Atmospheric pressure was measured using a Vaisala PTB101B (Scientific, 2017). Wind speed and direction were measured using an R. M. Young propeller and vane (Company, 2020). The precipitation reference sensor was a Geonor T-200B weighing bucket rain gauge (Geonor, 2010).

A4 Kucera and Steinson NOAA Testbed

The sensors used as reference sensors at the NOAA testbed of the Kucera and Steinson study were slightly different from the NCAR Marshall Field Site. Temperature and humidity were measured using a Technical Services Laboratory, Inc Hygrothermometer model 1088 (Laboratories, 2018). The vendor information provided accuracy results for the temperature, but the accuracy of the relative humidity measurements was not given. It is unclear if the accuracy of the system given for temperature is the same accuracy of the dew point temperature measurements. The uncertainty of the dew point measurements was found in an Atmospheric Radiation Measurement Program METTWR Handbook (Ritsche, 2006). The accuracy of the barometer was difficult to determine and information was found in a General Service Administration (GSA) schedule (Scientific, 2017). Wind speed and direction were measured using a Vaisala WS524 ultrasonic wind sensor (Vaisala, 2010). Precipitation was measured using the OTT all-weather precipitation accumulation weighing bucket gauge (White et al., 2004).

A5 Oklahoma Mesonet

The Oklahoma Mesonet deploys a R. M. Young Model 41342 temperature probe (Company, b) at 1.5 m (Mesonet, c). Relative humidity measurements are taken at 1.5 m (Mesonet, b) using a Vaisala HUMICAP HMP155 probe (Vaisala, 2019). Atmospheric pressure is measured using a Vaisala PTB220 digital barometer (Vaisala, 2005) and is housed in the data logger enclosure (Mesonet, a). Wind measurements are measured at ten meters (Mesonet, d) using a R. M. Young model 05103 propeller and vane wind monitor (Company, a). Rainfall is measured using a MetOne tipping bucket rain gauge (Mcpherson et al., 2007). A LI-COR pyranometer (Scientific, 1996) is used to measure downwelling global solar radiation (Mesonet, a).

Author contributions. Adam Theisen oversaw the general project, testing sensors, troubleshooting while at CIMMS. Final analysis of the data and development of the manuscript was performed by Adam Theisen at Argonne National Laboratory. Max Ungar and Bryan Sheridan were heavily involved throughout the life cycle of the project. They printed the components, developed the frame, built the wiring harnesses, assembled the weather station, performed site checks, and resolved problems while in the field. Bradley Illston provided insight and direction for deploying the instrument at the Mesonet site and general recommendations for the project.

Competing interests. The co-PI of the 3D-PAWS Initiative, Paul Kucera, was an advisor to Adam Theisen as an undergraduate student at the University of North Dakota.

Acknowledgements. The authors would like to acknowledge the Cooperative Institute of for Mesoscale Meteorological Studies (CIMMS) at the University of Oklahoma and their support of this research effort through the Director's Dedicated Directed Research Fund grant.

The authors We would like to thank Jamie Foucher from CIMMS, for handling all of our orders with ease. We would also like to acknowledge Paul Kucera and Martin Steinson at University Corporation for Atmospheric Research (UCAR) who along with the US National Weather Service International Activities Office (NWS IAO) launched the 3D-PAWS initiative Initiative and open-sourced the plans with support from the USAID Office of U.S. Foreign Disaster Assistance(OFDA).

. The authors would also like to acknowledge Brandt Smith, Tyler Thibodeau, and the Tom Love Innovation Hub at the University of Oklahoma for their support and use of their 3D printers, lab space, tools, and consumables. The project would not have been as successful without the use of their facilities.

The authors also Lastly, the authors acknowledge Alan Perry for his assistance in the design of the concrete feet footings to allow for the leveling of the frame.

Development of this manuscript was supported by the U.S. Department of Energy, Office of Science, under contract number DE-AC02-06CH11357.

References

AcuRite: PRO 5-in-1 Weather Station with HD Display and Lightning Detector, https://www.acurite.com/hd-display-with-5-in-1-weather-station-and-lightning-detector.html, 2019.

Allen, R. G., Pereira, L. S., Raes, D., Smith, M., et al.: Crop evapotranspiration-Guidelines for computing crop water requirements-FAO Irrigation and drainage paper 56, Fao, Rome, 300, D05 109, 1998.

Aponte-Roa, D. A., Montalvan, L. B., Velazquez, C., Espinoza, A. A., Velazquez, L. F., and Serrano, R.: Evaluation of a low-cost, solar-powered weather station for small-scale wind farm site selection, in: 2018 IEEE International Instrumentation and Measurement Technology Conference (I2MTC), IEEE, https://doi.org/10.1109/i2mtc.2018.8409853, http://dx.doi.org/10.1109/I2MTC.2018.8409853, 2018.

ARM: Oklahoma Mesonet (30OKM). 2018-08-15 to 2019-04-15, Southern Great Plains (SGP) External Data (satellites and others) (X1, https://adc.arm.gov/discovery/#v/results/s/finst::okm, 2019.

Aura, S., Muita, R., Oloo, P., Muchemi, D., Kucera, P., Mwangi, S., Maingi, N., Muigai, E., and Steinson, M.: Intercomparison of TAHMO, 3DPAWS Automatic Weather Stations and KMD's Dagoretti Corner, Nairobi Synoptic Weather Station Data, UK Met Office, https://www.metoffice.gov.uk/binaries/content/assets/metofficegovuk/pdf/business/international/wiser/wiser0170_highway_obs_data_intercomparison.pdf, 2019.

Brock, F. V., Crawford, K. C., Elliott, R. L., Cuperus, G. W., Stadler, S. J., Johnson, H. L., and Eilts, M. D.: The Oklahoma Mesonet: A Technical Overview, Journal of Atmospheric and Oceanic Technology, 12, 5–19, https://doi.org/10.1175/1520-0426(1995)012<0005:TOMATO>2.0.CO;2, https://doi.org/10.1175/1520-0426(1995)012<0005:TOMATO>2.0.CO;2, 1995.

Company, R. M. Y.: Wind Monitor Model 05103, http://www.youngusa.com/products/7/5.html, a.

Company, R. M. Y.: MODEL 41342 PLATINUM TEMPERATURE PROBE Instruction Sheet 41342-90, R. M. Young Company, http://www.mesonet.org/files/instruments/CSI_LI-200S.pdf, b.

Company, R. M. Y.: Heavy DutyWind Monitor-HD, http://www.youngusa.com/products/7/67.html, 2020.

DiCola, T.: Adafruit_Python_BMP, https://github.com/adafruit/Adafruit_Python_BMP, 2014a.

DiCola, T.: Adafruit_Python_MCP9808, https://github.com/adafruit/Adafruit_Python_MCP9808, 2014b.

Gaggero, M.: Adafruit_Python_HTU21D, https://github.com/mgaggero/Adafruit_Python_HTU21D, 2015.

Geonor: Geonor T-200B series All-weather precipitation gauges, http://geonor.com/datasheets/geonor-t200b-series-all-weather-precipitation-gauges.pdf, 2010.

Google: Google Earth Overview of 3D-Printed Weather Station Deployment Location, Accessed October 1, 2019, 2018.

Gutting, J.: Python_SI1145, https://github.com/THP-JOE/Python_SI1145, 2014.

Ham, J.: Using Arduinos and 3D-printers to Build Research-grade Weather Stations and Environmental Sensors, in: AGU 2013 Fall Meeting Abstracts, pp. H43H–1573, 2013.

Ham, J., Lloyd-Miner, G., Shonkwiler, K., and Nash, C.: Using 3D-printers and Low-cost Microcontroller Boards to Build Open-source Environmental Instrumentation, in: American Meteorological Society 2014 Annual Meeting, 2014.

Hoyer, S. and Hamman, J.: xarray: N-D labeled arrays and datasets in Python, Journal of Open Research Software, 5, https://doi.org/10.5334/jors.148, http://doi.org/10.5334/jors.148, 2017.

Hunter, J. D.: Matplotlib: A 2D graphics environment, Computing in Science & Engineering, 9, 90–95, https://doi.org/10.1109/MCSE.2007.55, 2007.

Inc, M. S.: HTU21D(F) Sensor Digital Relative Humidity sensor with Temperature output, Measurement Specialties Inc, https://cdn-shop.adafruit.com/datasheets/1899_HTU21D.pdf, 2013.

Kennedy, A.: A Low-Cost, Open-Source Snowflake Imager, in: American Meteorological Society 99th Annual Meeting, American Meteorological Society 99th Annual Meeting, Phoenix, AZ, https://ams.confex.com/ams/2019Annual/meetingapp.cgi/Paper/353304, 2019.

Kucera, P. and Steinson, M.: Development of Innovative Technology to Provide Low-Cost Surface Atmospheric Observations in Data Sparse Regions, in: EGU General Assembly Conference Abstracts, vol. 19, p. 11639, https://www.wmo.int/pages/prog/www/IMOP/AWS-conference/Papers/Topic_4/O4_1_Kucera_Development%20of%20Innovative%20Technology%20to%20provide%20low-cost%20observations.pdf, 2017a.

Kucera, P. A. and Steinson, M.: Development of Innovative Technology to Provide Low-Cost Surface Atmospheric Observations in Data Sparse Regions, https://www.wmo.int/pages/prog/drr/documents/mhews-ref/posters-pdfs/6.30-SteinsonKuceraLow-costsurfaceobsMHEWC2017poster.pdf, 2017b.

Kucera, P. A. and Steinson, M.: Calibration and Data Quality Assessment, https://sites.google.com/ucar.edu/3dpaws/home/calibration-and-data-quality-assessment, 2017c.

Laboratories, T. S.: Hygrothermometer | Weather Instruments from TSL, https://tslinc.com/systems/instruments-hygrothermometer/, 2018.

Mcpherson, R. A., Fiebrich, C. A., Crawford, K. C., Kilby, J. R., Grimsley, D. L., Martinez, J. E., Basara, J. B., Illston, B. G., Morris, D. A., Kloesel, K. A., and et al.: Statewide Monitoring of the Mesoscale Environment: A Technical Update on the Oklahoma Mesonet, Journal of Atmospheric and Oceanic Technology, 24, 301–321, https://doi.org/10.1175/jtech1976.1, 2007.

Mesonet, O.: Other Measurements, http://www.mesonet.org/index.php/site/about/other_measurements, a.

Mesonet, O.: Moisture Measurements, http://www.mesonet.org/index.php/site/about/moisture_measurements, b.

Mesonet, O.: Air Temperature and Related Measurements, http://www.mesonet.org/index.php/site/about/air_temperature_and_related_measurements, c.

Mesonet, O.: Wind Measurements, http://www.mesonet.org/index.php/site/about/wind_measurements, d.

Mesonet, O.: Site Viewer, http://www.mesonet.org/index.php/site/site_viewer/, 2013.

METER Group Inc, U.: All-in-one weather station, https://www.metergroup.com/environment/products/atmos-41-weather-station/, 2017a.

METER Group Inc, U.: ATMOS 41, http://library.metergroup.com/Manuals/20635_ATMOS41_Manual_Web.pdf, 2017b.

Ritsche, M.: Surface and Tower Meteorological Instrumentation at Atqasuk (METTWR2H) Handbook, Tech. rep., DOE Office of Science Atmospheric Radiation Measurement (ARM) Program . . . , 2006.

Scientific, C.: LI-COR LI200S Pyranometer Instruction Manual, Campbell Scientific Inc, http://www.mesonet.org/files/instruments/CSI_LI-200S.pdf, 1996.

Scientific, C.: CS105 - Vaisala PTB101B Barometer, https://www.campbellsci.com/cs105, 2017.

Scientific, C.: HC2S3-L - Temperature and Relative Humidity Probe, https://www.campbellsci.com/hc2s3, 2020.

Smallwood, D. J. and Santarsiero, R.: Evaluating 3D Printed Alternatives to Weather Monitoring, https://digitalcommons.wpi.edu/mqp-all/6659/, 2019.

Theisen, A.: Open source code and data from a 3D Printed Weather Station, https://doi.org/10.5281/zenodo.3820419, https://github.com/AdamTheisen/3DWxSt, 2019.

Theisen, A., Collis, S., Jackson, R., Sherman, Z., Hickmon, N. L., Kehoe, K. E., Godine, C., Sockol, A. J., King, A., and Giansiracusa, M. T.: Atmospheric Data Community Toolkit (ACT): A Python Library for Working with Atmospheric Data., in: 100th American Meteorological Society Annual Meeting, AMS, https://github.com/ARM-DOE/ACT, 2020.

Vaisala: PTB220 Digital Barometer, Seatronics Group, https://seatronics-group.com/files/5714/2072/1119/Vaisala_PTB220_Barometer_-_Datasheet.pdf, 2005.

Vaisala: WINDCAP Ultrasonic Wind Sensor WS425 User's Guide, Vaisala, 2010.

Vaisala: HUMICAP Humidity and Temperature Probe HMP155, Vaisala, https://www.vaisala.com/sites/default/files/documents/HMP155-Datasheet-B210752EN.pdf, 2019.

Virtanen, P., Gommers, R., Oliphant, T. E., Haberland, M., Reddy, T., Cournapeau, D., Burovski, E., Peterson, P., Weckesser, W., Bright, J., van der Walt, S. J., Brett, M., Wilson, J., Jarrod Millman, K., Mayorov, N., Nelson, A. R. J., Jones, E., Kern, R., Larson, E., Carey, C., Polat, İ., Feng, Y., Moore, E. W., Vand erPlas, J., Laxalde, D., Perktold, J., Cimrman, R., Henriksen, I., Quintero, E. A., Harris, C. R., Archibald, A. M., Ribeiro, A. H., Pedregosa, F., van Mulbregt, P., and Contributors, S. . .: SciPy 1.0: Fundamental Algorithms for Scientific Computing in Python, Nature Methods, 17, 261–272, https://doi.org/https://doi.org/10.1038/s41592-019-0686-2, 2020.

White, S. G., Winans, L., and Fiore, J.: Development of the all-weather precipitation accumulation gauge for ASOS, in: Preprints, Eighth Symp. on Integrated Observing and Assimilation Systems for Atmosphere, Oceans, and Land Surface, Seattle, WA, Amer. Meteor. Soc, vol. 7, 2004.

WMO: Guide to Instruments and Methods of Observation (WMO-No. 8), World Meteorological Organisation: Geneva, Switzerland, 1, https://library.wmo.int/doc_num.php?explnum_id=10179, 2018.

~~3D-printed weather station initial installation in the field.~~

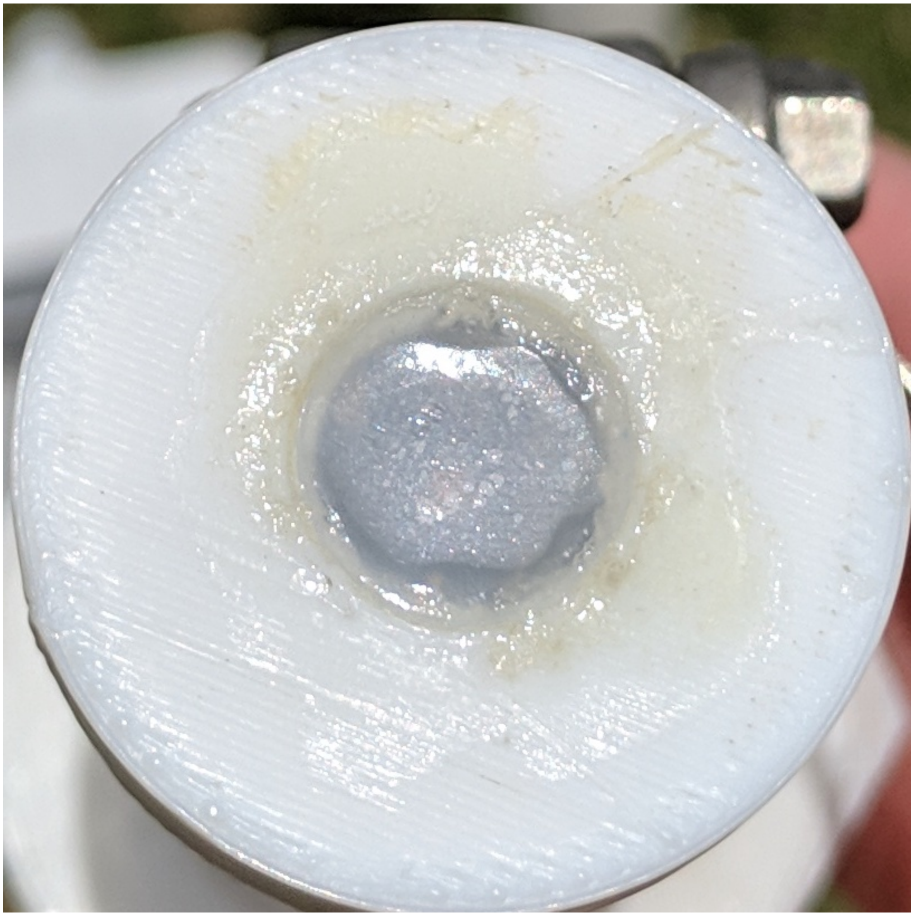

Figure 1. Ultraviolet index sensor using a plastic ~~disc~~ covering cut from a freezer meal tray. Image taken at the end of campaign shows yellowing of the glue used to seal the edges.

Figure 2. 3D-printed weather station upon initial installation in the field.

Figure 3. Location of the 3D-printed weather station relative to the Oklahoma Mesonet. Image courtesy of Google Earth (Google, 2018)

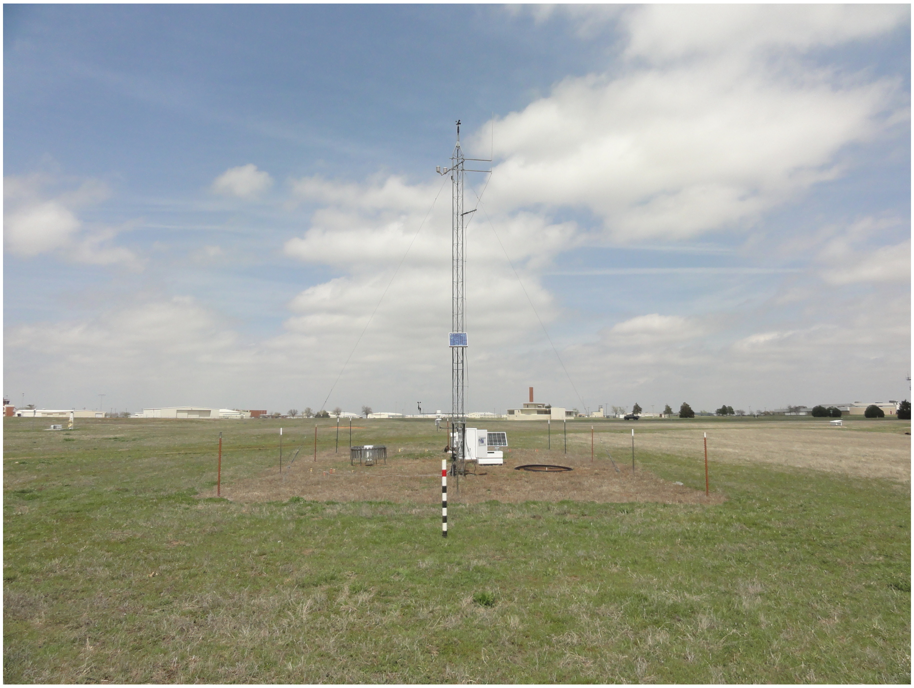

Figure 4. Norman Mesonet station from spring 2013. Image courtesy of the Oklahoma Mesonet (Mesonet, 2013)

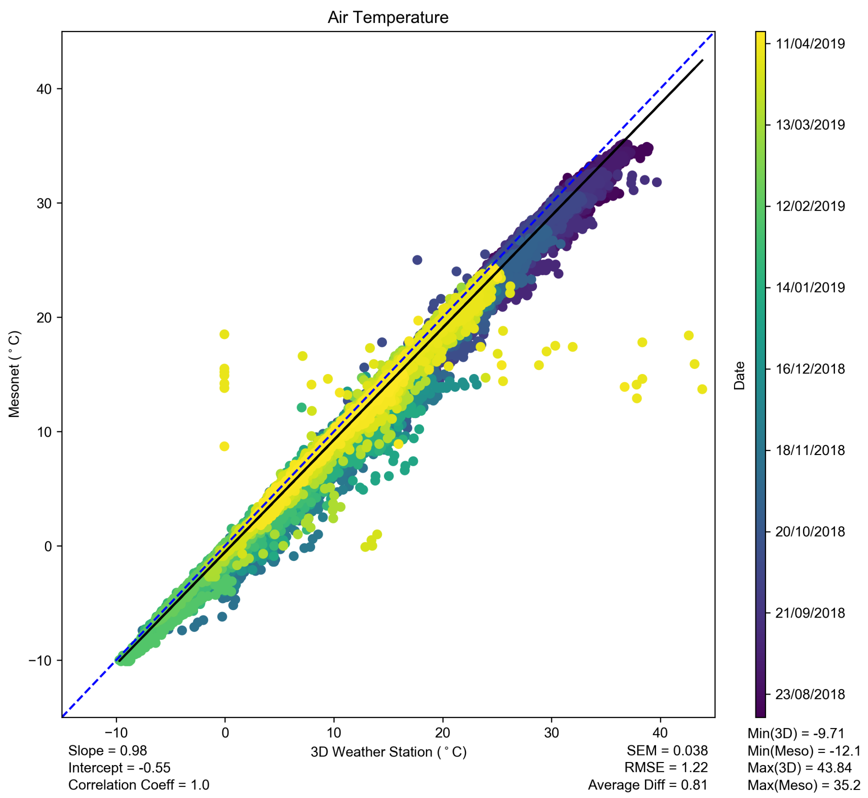

Figure 5. Comparison of the low-cost MCP9808 temperature sensor (x) and the Oklahoma Mesonet (y) for the entire deployment, color-coded by time.

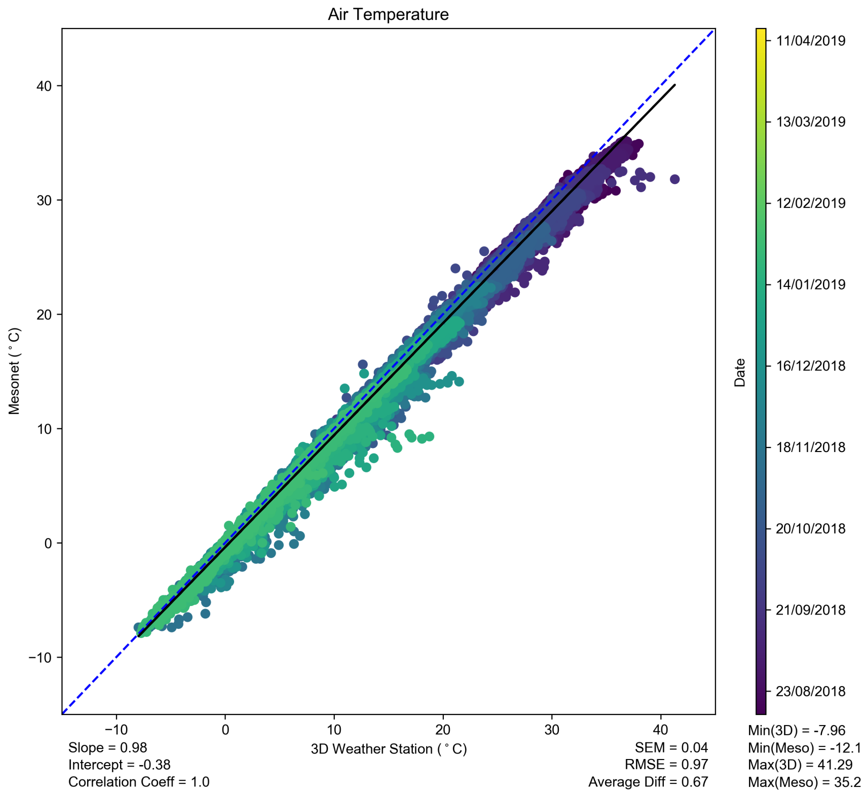

Figure 6. Comparison of the temperature from the low-cost HTU21D sensor (x) and the Oklahoma Mesonet (y) for six months of the ~~entire~~ deployment, color-coded by time.

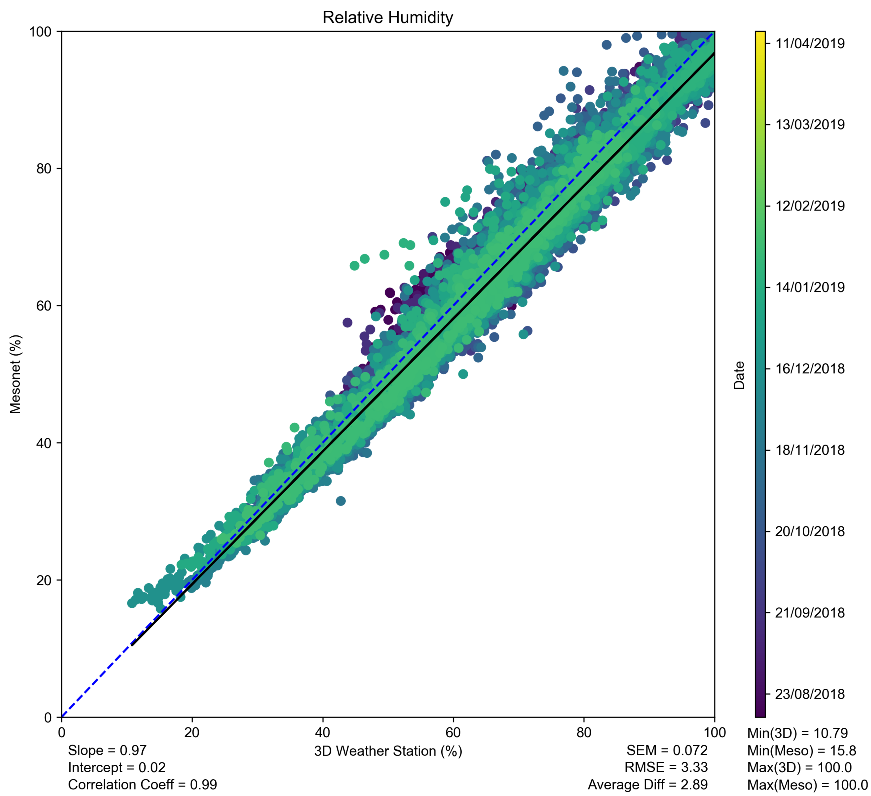

Figure 7. Comparison of the low-cost HTU21D relative humidity sensor (x) and the Oklahoma Mesonet (y) for ~~six-months~~ six months of the deployment, color-coded by time.

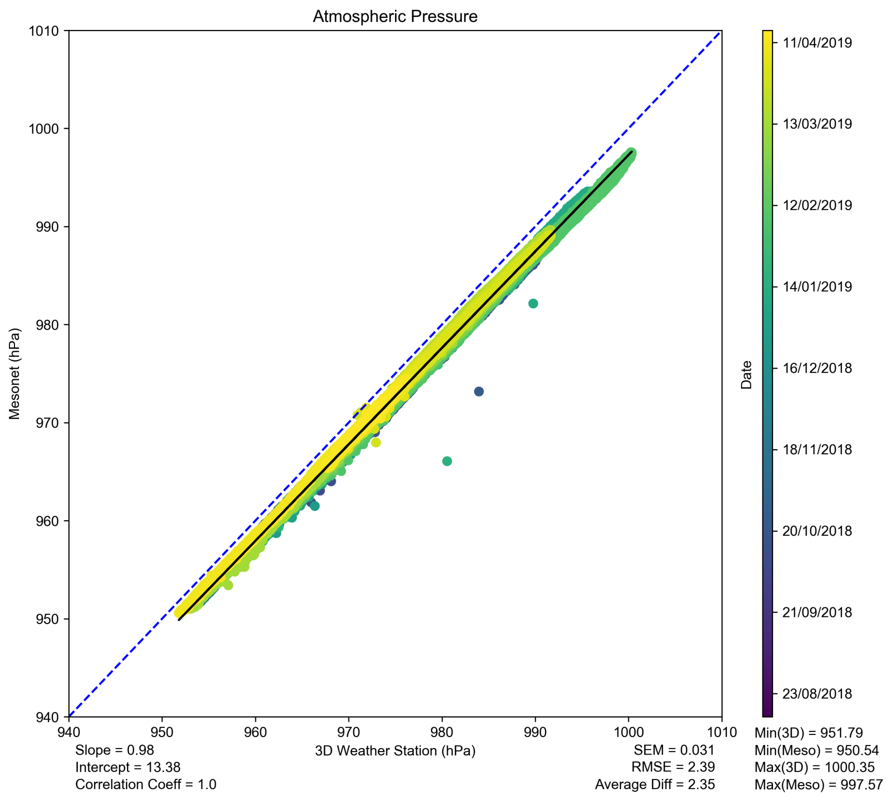

Figure 8. Comparison of the low-cost BMP280 pressure sensor (x) and the Oklahoma Mesonet (y) for seven months of the ~~entire~~ deployment, color-coded by time.

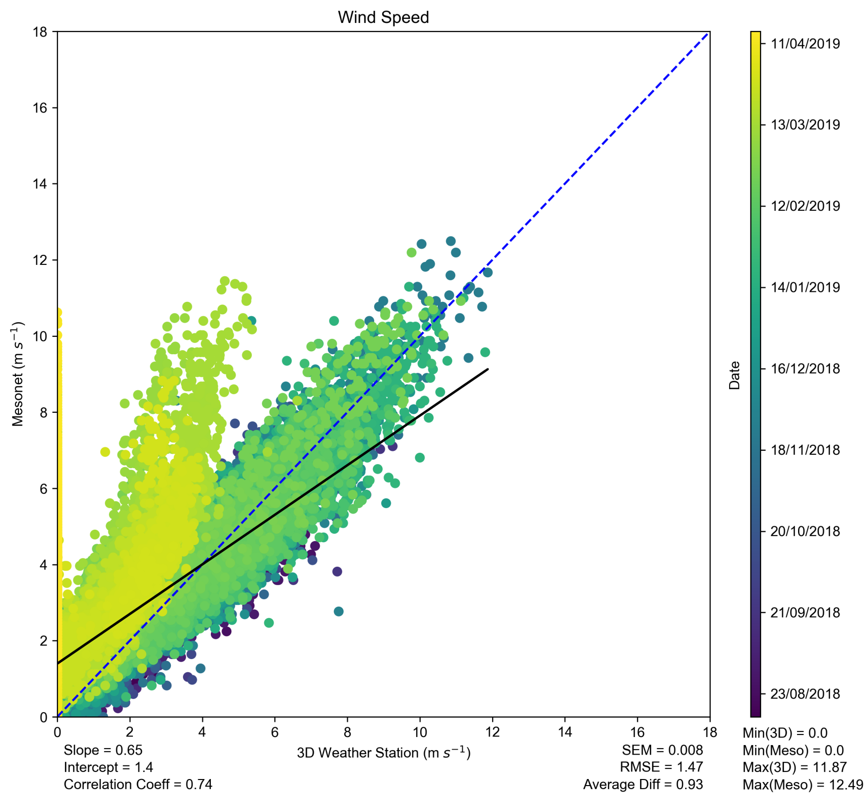

Figure 9. Comparison of the 3D-printed anemometer using a Hall effect sensor (x) and the Oklahoma Mesonet (y) for the entire deployment, color-coded by time.

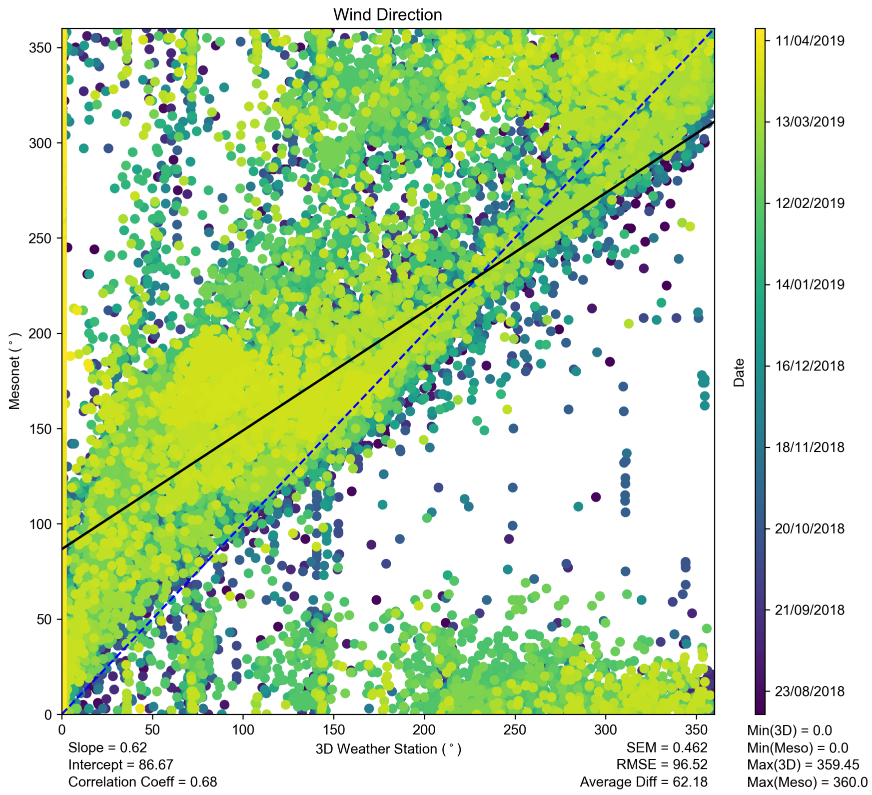

Figure 10. Comparison of the 3D-printed wind vane using a Hall effect rotary sensor (x) and the Oklahoma Mesonet (y) for the entire deployment, color-coded by time.

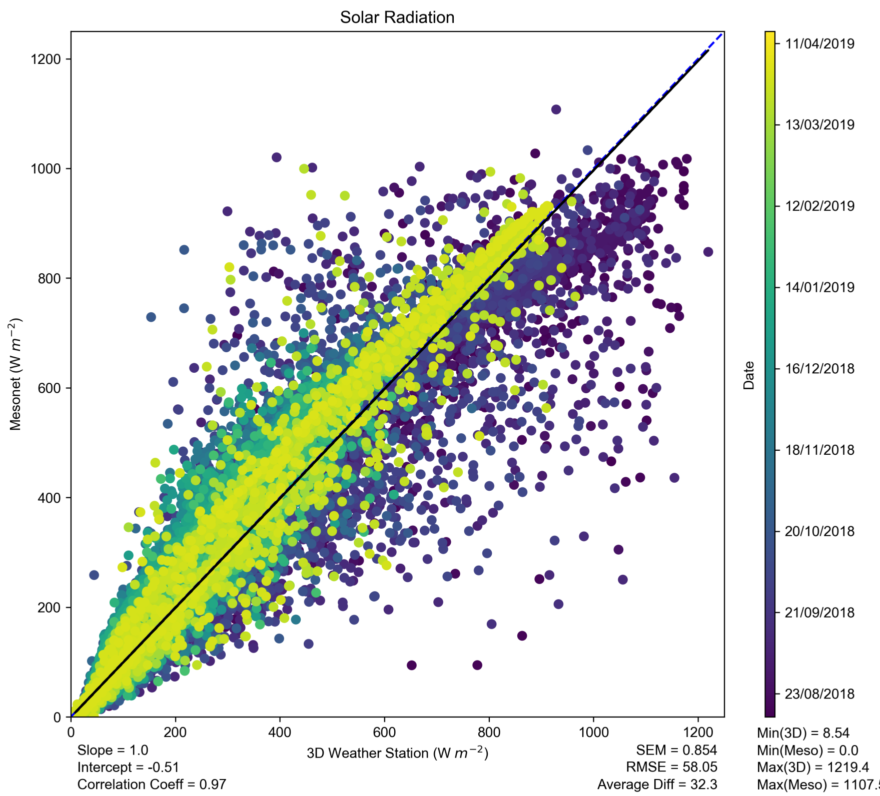

Figure 11. Comparison of the low-cost SI1145 UV sensor (x) and the Oklahoma Mesonet downwelling global solar radiation (y) for the entire deployment, color-coded by time.

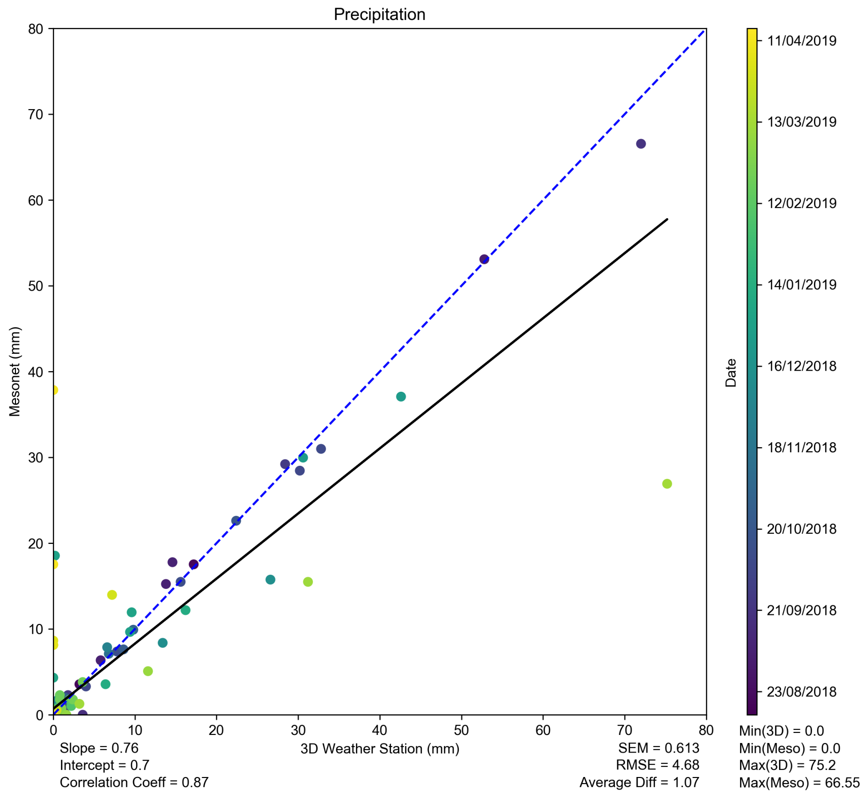

Figure 12. Comparison of the daily precipitation accumulations for the 3D-printed tipping bucket rain gauge using a Hall effect sensor (x) and the Oklahoma Mesonet (y) for the entire deployment, color-coded by time.

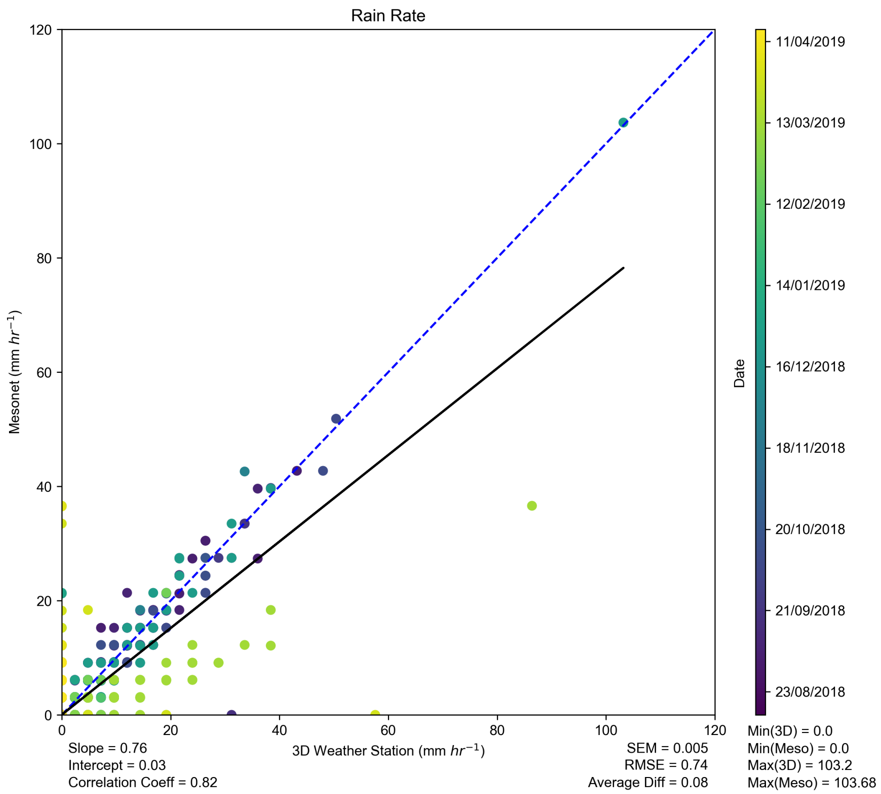

Figure 13. ~~3D-PAWS 10-month~~ Comparison of precipitation rates for the 3D-printed tipping bucket rain gauge using a Hall effect sensor ~~evaluation results (Kucera and Steinson, 2017c)~~(x) and the Oklahoma Mesonet (y) for the entire deployment, color-coded by time.

Table 1. 3D weather station sensor specifications

Parameter	Sensor	Range	Resolution	~~Uncertainty~~ Accuracy
Air Temperature ~~(~~	MCP9808	-40–125 °C ~~)~~	~~MCP9808~~ 0.0625 °C	~~0.1~~ ± 0.5 °C
~~Atmospheric Pressure (hPa)~~ Air Temperature	~~BMP280~~ HTU21D	~~0.1 hPa~~ -40–125 °C	0.01 °C	± ~~0.4 hPa~~ 0.3 °C (5–60 °C
Relative Humidity ~~(%)~~	HTU21D	~~1~~0–100 %	± 0.04 %	± 3 % (80–100 %) ± 2 % (0–80 %)
~~Wind Speed (m/s)~~ Atmospheric Pressure	BMP280	300–1100 hPa	0.16 hPa	± 1 hPa
Wind Speed	SS451A	unknown	0.1 m ~~/s~~ s^{-1}	unknown
Wind Direction ~~(deg)~~	Rotary ~~Sensor~~	0–360 °	1 ~~deg~~ °	unknown
UV Index ~~()~~	SI1145	~~0.01~~ unknown	~~Unknown~~ 0.282 ct lux^{-1}	unknown
Rainfall ~~(mm)~~	SS451A		0.2 mm	unknown

Wind speed resolution from Kucera and Steinson results

Mode definitions: I = Instantaneous measurement; A = Average over time; T = Total

Table 2. Oklahoma Mesonet Instrumentationinstrumentation (Mcpherson et al., 2007)

Parameter	Sensor	Accuracy Range	Resolution	Acc
Air Air Temperature (Temperature	RM Young 41342 RTD Probe	-50–50 °C (calibrated)	0.01 °C)	RM Young 41342 RTD P
Relative Atmospheric Pressure (mb) Humidity	Vaisala Barometer HMP155	± 0.4 mb 0–100 %	0.03 %	± 1 % (4 ± 0.6 %
Atmospheric Relative Humidity (%) Pressure	Vaisala HMP155 Barometer	500–1100 hPa	0.1 hPa	± 3%
Wind Speed (m /s)	RM Young RM Young Wind Monitor Wind Monitor	0–100 m s^{-1}	0.03 m s^{-1}	± 1 % or 0
Wind Wind Direction (deg) Direction	RM Young RM Young Wind Monitor Wind Monitor	0–360 °	0.05 °	± 3
Solar Solar Radiation Radiation	Li-Cor Pyranometer	0–3000 W m^{-2}	0.23 W m^{-2}	±
Rainfall (mm)	Met One TBRG		0.25 mm	1 % (2.5–7 at 2

Mode definitions: I = Instantaneous measurement; A = Average over time; T = Total

Temperature accuracy does not include the added uncertainty from the radiation shield

Table 3. Summary of reference instrument accuracy used in 3D-PAWS comparison studies, including requirements from WMO Guide to Instrument and Methods of Observation - Volume 1 Annex 1.A. (WMO, 2018)

Parameter	Smallwood & Santarsiero	Aura et al.	Kucera & Steinson NCAR Testbed	Kucera & Steinson NOAA Testbed	Oklahoma Mesonet	WMO Guidelines*
Air Temperature	1.1 °C	0.6 °C	0.1 °C at 23 °C	0.28 °C (-50–50 °C)	0.3 °C at 23 °C	0.1 °C (-40–40 °C) AMU: 0.2 °C
Relative Humidity	5 % (90–100 %) 4 % (80–90 %) 3 % (20–80 %) 4 % (10–20 %) 5 % (1–10 %)	4 % (90–100 %) 2 % (15–90 %)	0.8 % at 23 °C	Dewpoint Temperature 1 °C (-1–30 °C)	± 1 % (40–97 %) ± 0.6 % (0–40 %)	1 % AMU: 3 %
Atmospheric Pressure		1 hPa	0.5 hPa	0.1 hPa	0.2 hPa	0.1 hPa AMU: 0.15 hPa
Wind Speed	Accuracy in m s^{-1} 2.2 (<44 m s^{-1}) 1.8 (<22 m s^{-1}) 1.3 (<13 m s^{-1}) 0.9 (<4.5 m s^{-1})	3 %	Greater of 0.3 m s^{-1}or 3 %	Greater of 0.135 m s^{-1} or 3 %	Greater of 1 % or 0.3 m s^{-1}	0.5 m s^{-1} (<5 m s^{-1}) 10 % (> 5 m s^{-1}) AMU: Not Listed
Wind Direction		5 °	3 °	2 °	3 °	5 ° AMU: 5 °
Solar Radiation	NA	5 %	NA	NA	5 %	2 % AMU: Daily: 5 % AMU: Hourly 8 %
Rainfall	5 %	5 %	0.1 % FS	4 %	1 % (2.5–7.6 cm hr^{-1}) at 21 °C	0.1 mm (<5mm) 2 % (> 5mm) AMU: Greater of 5 % or 0.1 mm

AMU: WMO Achievable Measurement Uncertainty

* - WMO Guide to Instruments and Methods of Observation, Volume 1 - Measurement of Meteorological Variables, Annex 1.A (WMO, 2018)

Information was retrieved from a number of sources, see Appendix A for details

Temperature accuracy does not include the added uncertainty from the radiation shield

Table 4. Comparison statistics summary of RMSE (top value) and correlation coefficient (bottom value)

Parameter	Month 1 15 Aug 2018	Month 2 16 Sep 2018	Month 3 16 Oct 2018	Month 4 16 Nov 2018	Month 5 16 Dec 2018	Month 6 16 Jan 2019	Month 7 16 Feb 2019	Month 8 16 Mar 2019	Entire Period
MCP Air Temperature (°C)	1.32 0.98	1.06 0.99	1.26 0.99	1.33 0.99	1.20 0.99	0.90 0.99	0.42 1.00	1.53 0.98	1.22 1.00
HTU Air Temperature (°C)	1.11 0.99	0.94 0.99	0.96 1.00	0.99 0.99	0.85 0.99	1.00 0.99			0.97 1.00
Relative Humidity (%)	2.63 0.99	3.38 0.99	3.73 0.99	3.42 0.99	3.45 0.99	3.09 0.99			3.33 0.99
Atmospheric Pressure (hPa)		2.92 1.00	2.51 1.00	2.21 1.00	2.44 1.00	2.60 1.00	2.41 1.00	1.90 1.00	2.39 1.00
Wind Speed ($m\ s^{-1}$)	0.58 0.92	0.56 0.94	0.59 0.95	0.67 0.95	0.69 0.94	0.88 0.94	2.49 0.67	2.98 0.29	1.47 0.74
Wind Direction (°)	79.74 0.60	68.03 0.75	80.13 0.80	95.02 0.74	87.16 0.78	118.58 0.42	94.49 0.73	130.27 0.63	96.52 0.68
Solar Radiation ($W\ m^{-2}$)	81.64 0.98	68.77 0.96	50.86 0.98	52.35 0.99	44.49 0.98	34.14 0.99	34.23 0.99	54.22 0.99	58.05 0.97
Rainfall Daily Total (mm)	0.65 1.00	1.32 1.00	0.27 1.00	2.21 0.98	3.79 0.92	0.26 0.89	9.87 0.98	8.02 0.25	4.68 0.87
Rain Rate ($mm\ hr^{-1}$)	0.42 0.96	0.61 0.94	0.35 0.87	0.34 0.86	0.69 0.91	0.20 0.33	1.27 0.88	1.25 0.01	0.74 0.82

Date indicated in first row is the start date of the period used in the analysis.

Table 5. 3D weather station temperature RMSE (top value) and correlation coefficient (bottom value) response to increased wind speeds thresholds

Sensor	0 m s^{-1}	1 m s^{-1}	2 m s^{-1}	3 m s^{-1}	4 m s^{-1}	5 m s^{-1}	6 m s^{-1}	7 m s^{-1}	8 m s^{-1}
MCP9808 Temperature (°C)	1.22 1.00	1.08 1.00	1.01 1.00	0.94 1.00	0.88 1.00	0.75 1.00	0.60 1.00	0.54 1.00	0.51 1.00
HTU21D Temperature (°C)	0.97 1.00	0.91 1.00	0.87 1.00	0.83 1.00	0.77 1.00	0.65 1.00	0.50 1.00	0.43 1.00	0.47 1.00
HTU21D Relative Humidity (%)	3.33 0.99	3.35 0.99	3.28 0.99	3.27 1.00	3.33 1.00	3.41 1.00	3.56 1.00	3.59 1.00	3.49 1.00

Table 6. Maximum precipitation rate and daily accumulations recorded each month

Parameter	Month 1 15 Aug 2018	Month 2 16 Sep 2018	Month 3 16 Oct 2018	Month 4 16 Nov 2018	Month 5 16 Dec 2018	Month 6 16 Jan 2019	Month 7 16 Feb 2019	Month 8 16 Mar 2019
Mesonet Accumulation (mm)	53.1	66.6	22.6	15.8	37.1	1.8	26.9	37.9
3D-Printed Accumulation (mm)	52.8	72.0	22.4	26.6	42.6	2.2	75.2	7.2
Mesonet Rain Rate (mm hr^{-1})	42.7	51.8	27.5	42.6	103.7	6.1	36.6	36.6
3D-Printed Rain Rate (mm hr^{-1})	43.2	50.4	26.4	33.6	103.2	7.2	86.4	57.6